Chapter 14

Space Weather and the Vulnerability of Electric Power Grids

An Overview of the Increasing Vulnerability Trends of Modern Electric Power Grid Infrastructures and the potential consequences of Extreme Space Weather Environments

John G. Kappenman

Metatech Corporation, Applied Power Solutions Division
5 W. First St, Suite 301, Duluth, Mn, USA

Abstract A number of trends are causing overall increases in geomagnetically-induced currents (GIC's) and associated threats from geomagnetic storms for electric power grids. GIC threats have been a concern for power grids at high-latitude locations due to disturbances driven by electrojet intensifications. However, other geomagnetic storm processes such as SSC and ring current intensifications are also proving to cause GIC concerns for the power industry at low-latitude locations as well. In addition to threats arising from various regions of the space environment, the response of local ground and power system design have important roles that can significantly increase risk from geomagnetic storms. In particular a number of long-term trends in power system design and operation have been continually acting to increase geomagnetic storm risks. These design implications have acted to greatly escalate GIC risks for power grids at all latitude locations. As a result, GIC impacts may now be of concern even to power grids that have never considered the risk of GIC previously because they were not at high latitude locations. The paper will provide a comprehensive overview of these risk issues as they apply to many world power systems and particularly review the potential impacts to power system operations due to extreme geomagnetic disturbance events.

Keywords Geomagnetically induced currents, GIC, geoelectric field, geomagnetic disturbances, electric power grids, reactive power demand, MVARs, harmonics, SSC, electrojet intensification, ring current intensification.

I.A. Daglis (ed.), Effects of Space Weather on Technology Infrastructure, 257-286.

1. INTRODUCTION

Continuous advances have occurred in the understanding of space weather or more specifically geomagnetic storm environments and the ability of modelling these environments and the environmental interactions with electric power networks. As these efforts have progressed, it has also become evident that devastating impacts due to these storms events are plausible. These disturbances have caused catastrophic impacts to technology systems in the past (e.g., the power blackout in Quebec in March 1989). More importantly, as detailed examinations have been undertaken concerning the interaction of geomagnetic storm environments with power grids and similar infrastructures, the realization has developed that these infrastructures are becoming more vulnerable to disruption from electromagnetic interactions for a wide variety of reasons. This direction of these trends suggests that even more severe impacts can occur in the future for reoccurrences of historically large storms on present-day systems.

While more details will be provided in later sections of this paper, a brief overview of how these geomagnetic disturbance environments actually interact with large regional power grids indicates the complex nature of the threat. When geomagnetic storms occur they result in slowly varying (1-1000 seconds) geomagnetic field disturbances that can have very large geographic footprints. These magnetic field disturbances will induce electric fields at the Earth's surface over these same large regions. Across the U.S. and most other locations around the world, complex topologies of long-distance transmission lines have been built. These grids include transformers at generating plants and substations that have grounded neutrals. The transformer neutrals provide a path from the network to ground for these slowly varying electric fields (less than 1 Hz) to induce a current flow through the network phase wires and transformers.

These currents (known as geomagnetically-induced currents – GICs) are generally on the order of 10s to 100s of amperes during a geomagnetic storm. Though these quasi-DC currents are small compared to the normal AC current flows in the network, they have an impact that becomes enormously amplified on the operation of transformers in the network. Under normal conditions, even the largest transformer requires only a few amperes of AC excitation current to energize its magnetic circuit. GIC when present, also acts as an excitation current for these magnetic circuits, therefore GIC levels of only 1 to 10 amperes can initiate magnetic core saturation during one-half of the AC cycle in an exposed transformer, causing extremely large AC currents to be drawn from the power grid. As GIC levels increase, the levels of saturation of the transformer core also increase.

When a transformer saturates due to the presence of GIC, it effectively becomes an amplifier of highly distorted AC current. Because the disturbance can span a very large area, this large injection of AC distortion behaviour can be produced simultaneously in a large number of exposed transformers. The simultaneous injections of these AC distortions from many transformers can cause widespread operational and reliability problems throughout the grid. This amplified AC current from saturation effects can pose risks to power networks directly due to increased reactive power demands that can lead to voltage regulation problems. But a nearly equal concern arises from collateral impacts stemming from highly distorted waveforms (rich in harmonics) from saturated transformers that are injected into the network. These distortions can cascade problems by disrupting the performance of other network apparatus and causing them to trip off-line just when they are most needed to preserve network integrity (i.e. relay & protection system mis-operation). If the spatial coverage of the disturbance is large, many transformers will be simultaneously saturated, a situation that can rapidly escalate into a network-wide voltage collapse. In addition, individual transformers may be damaged from overheating due to this unusual mode of operation, which can result in long-term outages to key transformers in the network. In short, the threats to the infrastructure from geomagnetic storms include the possibility of widespread power blackouts, damage to expensive and difficult to replace transformers, and damage to equipment connected to the grid.

In order to assess the risks that modern electric power grids face in regards to the space environment it is necessary to consider a wide variety of risk modifiers and multipliers. These risk modifiers start with a consideration of the various space environment disturbance processes that can cause differing degrees of impulsive geomagnetic disturbance environments at differing latitude locations from auroral locations to equatorial locations. Other risk modifiers include the nature of the electromagnetic interaction between geomagnetic field disturbances and the solid-earth geophysics of the terrestrial environment that produces the geo-electric field. This particular risk modifier may be responsible for the highest degree of uncertainty because of the relative lack of information on the conductivity properties to depth of many regions of the Earth. And finally what is emerging as one of the largest risk escalators for electric power grids, is the greatly magnified exposure risks due to geomagnetic storms, which has developed from the evolution of power grid design and operational factors.

2. GEOLOGICAL RISK FACTORS & GEO-ELECTRIC FIELD RESPONSE

Considerable prior work has been done to model the geomagnetic induction effects in ground-based systems [Albertson, Lanzerotti-1983, Pirjola]. As an extension to this fundamental work, numerical modelling of ground conductivity conditions have been demonstrated to provide accurate replication of observed geo-electric field conditions over a very broad frequency spectrum [Kappenman-1997]. Past experience has indicated that 1-D Earth conductivity models are sufficient to compute the local electric fields. Lateral heterogeneity of ground conductivity conditions can be significant over meso-scale distances [Kappenman-2001]. In these cases, multiple 1-D models can be used in cases where the conductivity variations are sufficiently large.

Ground conductivity models need to accurately reproduce geo-electric field variations that are caused by the considerable frequency ranges of geomagnetic disturbance events from the large magnitude/low frequency electrojet-driven disturbances to the low amplitude but relatively high frequency impulsive disturbances commonly associated with SSC events. This variation of electromagnetic disturbances therefore require models accurate over a frequency range from 0.3 Hz to as low as 0.00001 Hz. At these low frequencies of the disturbance environments, diffusion aspects of ground conductivities must be considered to appropriate depths. Therefore skin depth theory can be used in the frequency domain to determine the range of depths that are of importance. It is clear that for constant Earth conductivities, the depths required are more than several hundred kilometres, although the exact depth is a function of the layers of conductivities present at a specific location of interest.

It is generally understood that the Earth's mantle conductivity increases with depth. In most locations, ground conductivity laterally varies substantially at the surface over meso-scale distances; these conductivity variations with depth can range 3 to 5 orders of magnitude. While surface conductivity can exhibit considerable lateral heterogeneity, conductivity at depth is more uniform, with conductivities ranging from values of .1 to 10 S/m at depths from 600 to 1000km [Campbell-1987, Masse-1987]. If sufficient low-frequency measurements are available to characterize ground conductivity profiles, models of ground conductivity can be successfully applied over meso-scale distances and can be accurately represented by use of layered conductivity profiles or models. For illustration of the importance of ground models on the response of geo-electric fields, a set of four example ground models have been developed that illustrate the probable

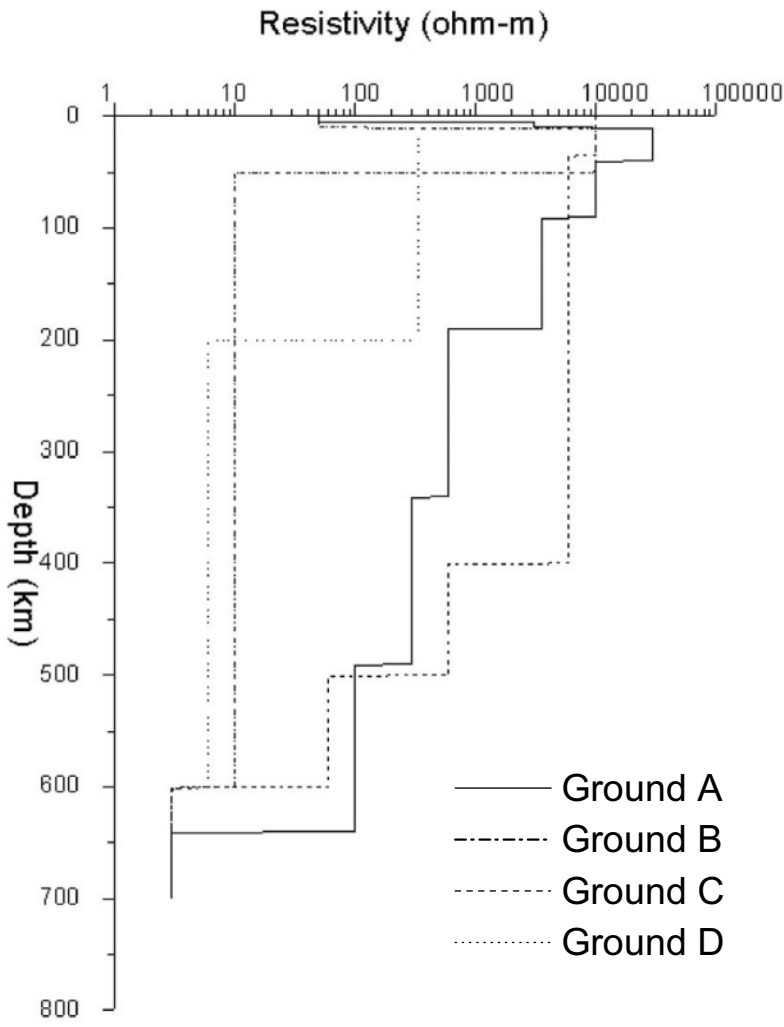

Figure 1. Resistivity profiles versus depth for four example layered earth ground models.

lower to upper quartile response characteristics of most known ground conditions, considering there is a high degree of uncertainty in the plausible diversity of upper layer conductivities. Figure 1 provides a plot of the layered ground conductivity conditions for these four ground models to depths of 700 km. As shown, there can be as much as four orders of magni-

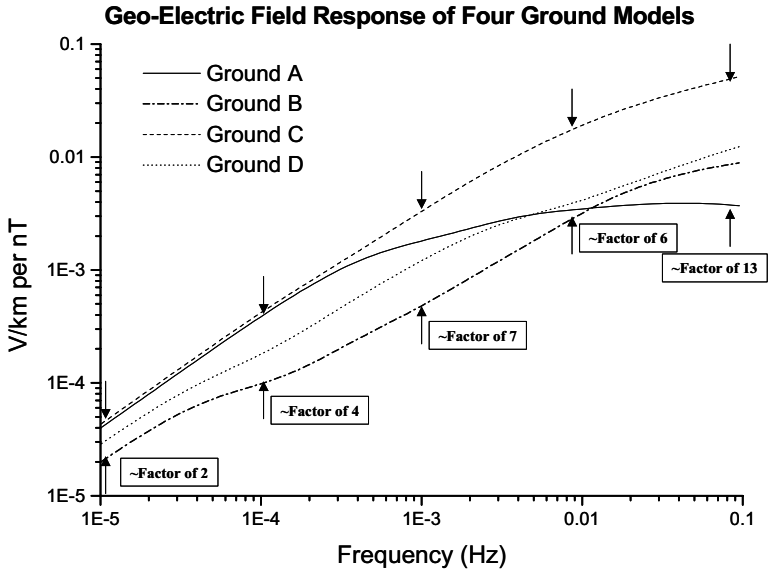

Figure 2. Frequency response of four example ground models of Figure 1, Max/Min geo-electric field response characteristics shown at various discrete frequencies.

tude variation in ground resistivity at various depths in the upper layers. Models A and B have very thin surface layers of relatively low resistivity. Models A and C are characterized by levels of relatively high resistivity until reaching depths exceeding 400km, while models B and D have high variability of resistivity in only the upper 50 to 200km of depth [Campbell-1980, Rasmussen-1987, 1988].

Figure 2 provides the frequency response characteristics for these same four layered earth ground models of Figure 1. Each line plot represents the geo-electric field response for a corresponding incident magnetic field disturbance at each frequency. While each ground model has unique response characteristics at each frequency, in general all ground models produce higher geo-electric field responses as the frequency of the incident disturbance increases. Also shown on this plot are the relative differences in geo-electric field response for the lowest and highest responding ground model at each decade of frequency. This illustrates that the response between the lowest and highest responding ground model can vary at discrete frequencies by more than a factor of 10. Also because the frequency content of an impulsive disturbance event can have higher frequency content (for instance due to a SSC), the disturbance is acting upon the more responsive portion of the frequency range of the ground models [Kappenman-2003].

Therefore, the same disturbance energy input at these higher frequencies produces a proportionately larger response in geo-electric field. For example in most of the ground models, the geo-electric field response is a factor of 50 higher at 0.1 Hz compared to the response at 0.0001 Hz.

From the frequency response plots of the ground models as provided in Figure 2, some of the expected geo-electric field response due to geomagnetic field characteristics can be inferred. For example, Ground C provides the highest geo-electric field response across the entire spectral range, therefore, it would be expected that the time-domain response of the geo-electric field would be the highest for nearly all B field disturbances. At low frequencies, Ground B has the lowest geo-electric field response while at frequencies above 0.02 Hz, Ground A produces the lowest geo-electric field response. Because each of these ground models have both frequency-dependent and non-linear variations in response, the resulting form of the geo-electric field waveforms would be expected to differ in form for the same B field input disturbance. In all cases, each of the ground models produces higher relative increasing geo-electric field response as the frequency of the incident B field disturbance increases. Therefore it should be expected that a higher peak geo-electric field should result for a higher spectral content disturbance condition.

A large electrojet-driven disturbance is capable of producing an impulsive disturbance as shown in Figure 3, which reaches a peak delta B magnitude of ~2000 nT with a rate of change (dB/dt) of 2400 nT/min. This disturbance scenario can be used to simulate the estimated geo-electric field response of the four example ground models. Figure 4 provides the geo-electric field responses for each of the four ground models for this 2400 nT/min B field disturbance. As expected, the Ground C model produces the largest geo-electric field reaching a peak of ~15 V/km, while Ground A is next largest and the Ground B model produces the smallest geo-electric field response. The Ground C geo-electric field peak is more than 6 times larger than the peak geo-electric field for the Ground B model. It is also evident that significant differences result in the overall shape and form of the geo-electric field response. For example, the peak geo-electric field for the Ground A model occurs 17 seconds later than the time of the peak geo-electric field for the Ground B model. In addition to the differences in the time of peak, the waveforms also exhibit differences in decay rates. As is implied from this example, both the magnitudes of the geo-electric field responses and the relative differences in responses between models will change dependent on the source disturbance characteristics.

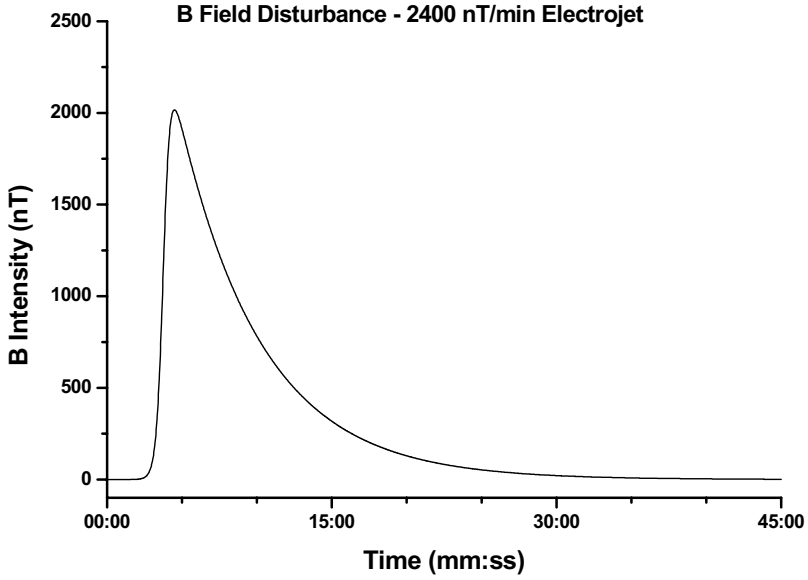

Figure 3. Waveform of example electrojet-driven geomagnetic field disturbance with 2400 nT/min rate of change intensity.

3. POWER GRID DESIGN & NETWORK TOPOLOGY RISK FACTORS

While ground conductivity conditions are important in determining the geo-electric field response, and in determining levels of GICs and their resulting impacts. Power grid design is also an important factor in the vulnerability of these critical infrastructures, a factor in particular that over time has greatly escalated the effective levels of GIC and operational impacts due to these increased GIC flows.

Power systems are designed and operated with a focus on maintaining a balance between generation and demand at all times in a distributed manner. Sufficient reserves are provided throughout the system so that it can tolerate the loss of any one component at any time (the N-1 criterion). Power system designers and operators expect these systems to be challenged by the elements, and where those challenges were fully understood in the past, the system design has worked extraordinarily well.

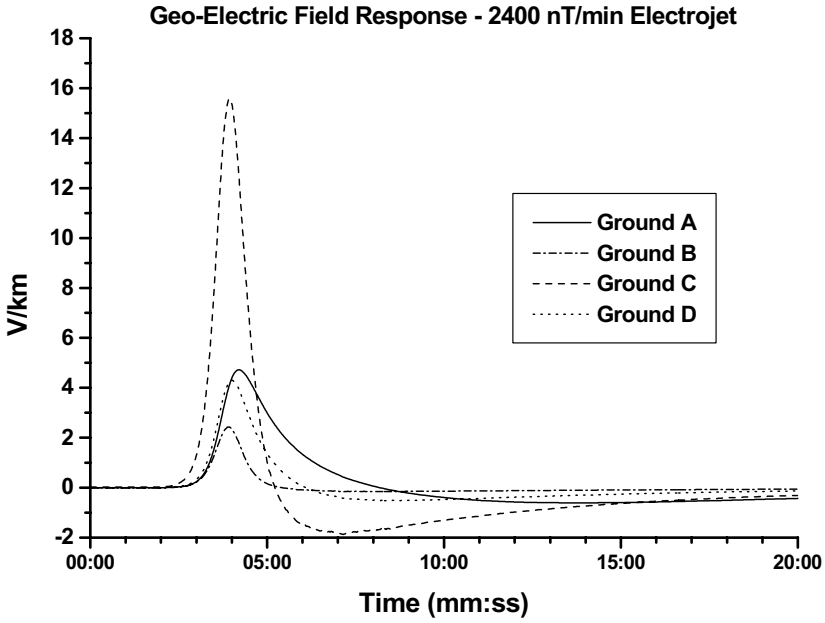

Figure 4. Geo-electric field response of the four example ground models to the 2400 nT/min disturbance conditions of Figure 3.

The primary design approach undertaken by the industry for decades has been to weave together a tight network, which pools resources and provides redundancy to reduce failures. In essence, unaffected neighbouring grids help out the temporarily weakened portion of the grid.

Ironically, the designs that have worked to make the electric power industry strong for ordinary weather, introduce key vulnerabilities to the electromagnetic coupling phenomena of geographically widespread geomagnetic disturbances. Since large interconnected power grids and intense geomagnetic disturbances can both have continental footprints, the design concept of unaffected neighbouring system and sharing the burden of storm-caused stresses are not always realizable. Unlike ordinary weather patterns that arise due to thermodynamic conditions, the electromagnetic interactions of impulsive geomagnetic field disturbances can develop very rapidly and when present are inherently near-instantaneously observed across the exposed system.

The extent of the change or growth in vulnerability in the US and other major world power grid infrastructures over time are due to a number of factors stemming from either growth in the infrastructure base or technology changes within the existing base that introduce new impact problems.

Figure 5 shows the growth of the US high voltage transmission grid over the last 50 years. The high voltage transmission grid is the portion of the power network that spans long distances. This geographically widespread infrastructure readily couples through multiple ground points to the geo-electric field produced by disturbances in the geomagnetic field. As shown in Figure 5, from Solar Cycle 19 (late 1950's), through Solar Cycle 22 (early 1980's), the high voltage transmission grid has grown nearly tenfold. Similar development rates of transmission infrastructure have occurred simultaneously in other developed regions of the world.

As this network has grown in size, it has also grown in complexity and sets in place a compounding of risks that are posed to the US power grid infrastructure for GIC events. Some of the more important changes in technology base that can increase impacts from GIC events include higher design voltages, changes in transformer design and other related apparatus. The operating levels of high-voltage networks have increased from the 100-200kV thresholds of the 1950's to 400 to 765kV levels of present-day networks. With this increase in operating voltages, the average per unit length circuit resistance has decreased while the average length of the grid circuit increases. In addition, power grids are designed to be tightly interconnected networks, which present a complex and in many cases a system that is continental in size. These interrelated design factors have acted to substantially increase the levels of GIC that are possible in modern power networks.

All high voltage bulk power grids throughout the world utilize a three-phase configuration for delivery of power over the long-distance high voltage transmission networks from power generation facilities to end-users of the electricity. In this delivery process, transformers are used to step up or step-down voltage levels, as it is most efficient to transmit long distances at high voltage (69kV to 765kV), but producing and using electricity has to be done at very low voltages (120 to 4000 volts). These transformers introduce the path by which GIC enters and exits the power grid. Also, the GIC when it flows through these transformers is the root cause of all power system problems as these transformers saturate due to this quasi-DC current. This saturated mode of operation can cause distortions or disruptions to the operation of the entire power grid.

GIC levels are determined by the size and the resistive impedance of the power grid circuit itself when coupled with the level of geo-electric field that results from the geomagnetic disturbance event. Given a geo-electric field imposed over the extent of a power grid, a current will be produced entering the neutral ground point at one location and exiting through other ground points elsewhere in the network.

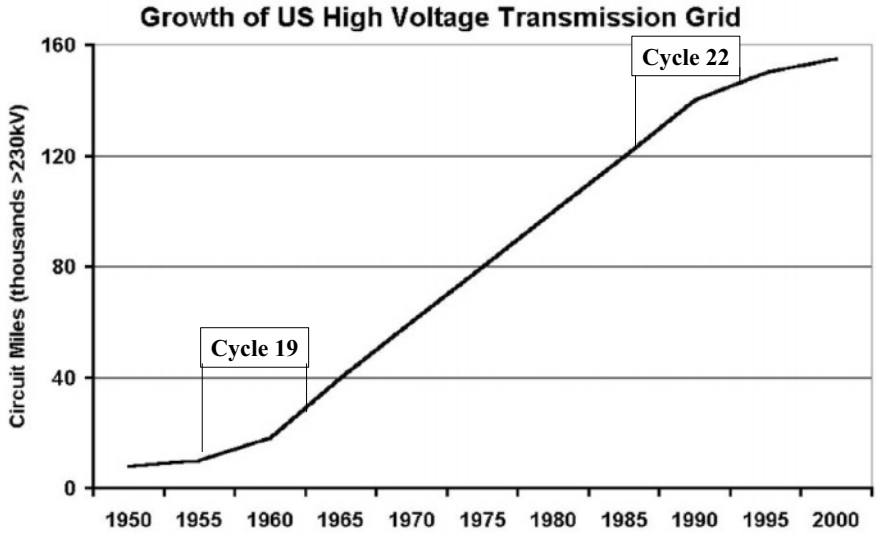

Figure 5**.** Growth of the US High Voltage Transmission Network over the past 50 years.

The resistive impedance of transmission circuits vary significantly with voltage class, the higher the kV rating the lower the resistive impedance per unit distance (i.e. ohms per mile) [Howlett, ECAR, FERC]. Figure 6 provides a plot of the average resistive impedance per transmission line by the major kV Rating classes for the US power grid. The lowest transmission system voltage surveyed was at 69kV, while the highest was at 765kV. As indicated, the average R per unit length decreases by more than a factor of 10 as the voltage level increases over this range. Therefore a 69kV and 765kV transmission lines of equal length will also have factor of ~10 difference in total circuit resistance and if coupled to the same geo-electric field, the level of GIC flow will be ~10 times larger in the 765kV line.

The resistive impedance of transformers exhibits an even larger degree of decrease as the size rating of the transformer increases. Figure 7 provides a plot of transformer R versus the AC Current Rating. As shown in this plot, a sampling of the actual data points for transformers in the US population are shown along with population data, which indicates a factor of 20 reduction in R as the transformer size increases. As shown in this plot, a sampling of the actual data points for transformers in the US population are shown along with population data, which indicates a factor of 20 reduction in R as the transformer size increases. When this resistive element is added to the

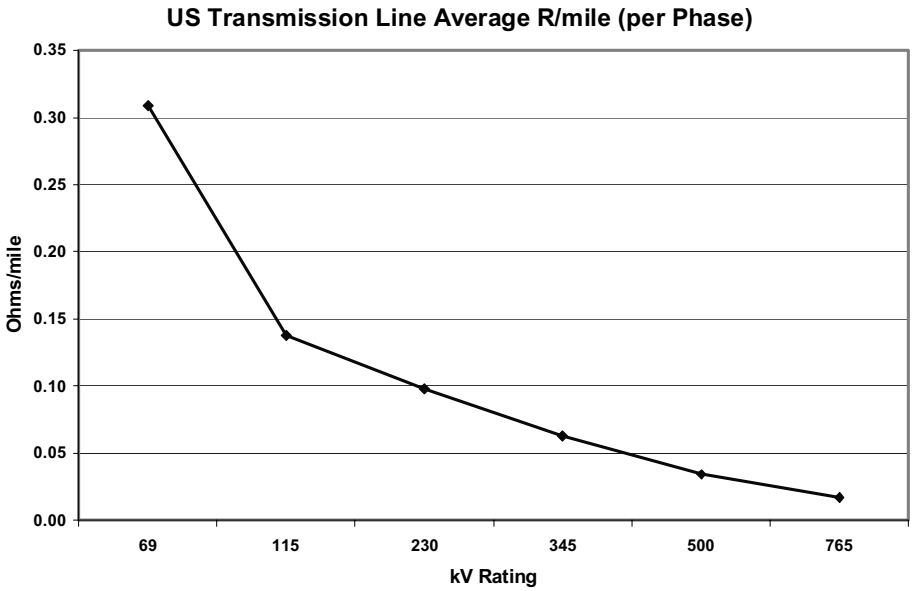

Figure 6. Average transmission line resistance per mile in the US by kV rating of the transmission lines.

overall GIC circuit, the expected trend should be a large increase in GIC levels for higher kV ratings.

This trend, of course, has ominous implications in that larger GIC flows will occur on the larger and more important portions of the power grid infrastructure. Most power grids are highly complex networks with numerous circuits or paths and transformers for GIC to flow through. This requires the application of highly sophisticated network and electromagnetic coupling models to determine the magnitude and path of GIC throughout the complex power grid. However for the purposes of illustrating the impact of power system design, a review will be provided using a single transmission line terminated at each end with a single transformer to ground connection. To illustrate the differences that can occur in levels of GIC flow at higher voltage levels, the simple demonstration circuit have also been developed at 138kV, 230kV 345kV, 500kV and 765kV which are common grid voltages used in the US and Canada. In Europe, voltages of 130kV, 275kV and 400kV are commonly used for the bulk power grid infrastructures. For these calculations, a uniform 1.0 volt/km geo-electric field disturbance conditions are used, which means that the change in GIC levels will result from changes

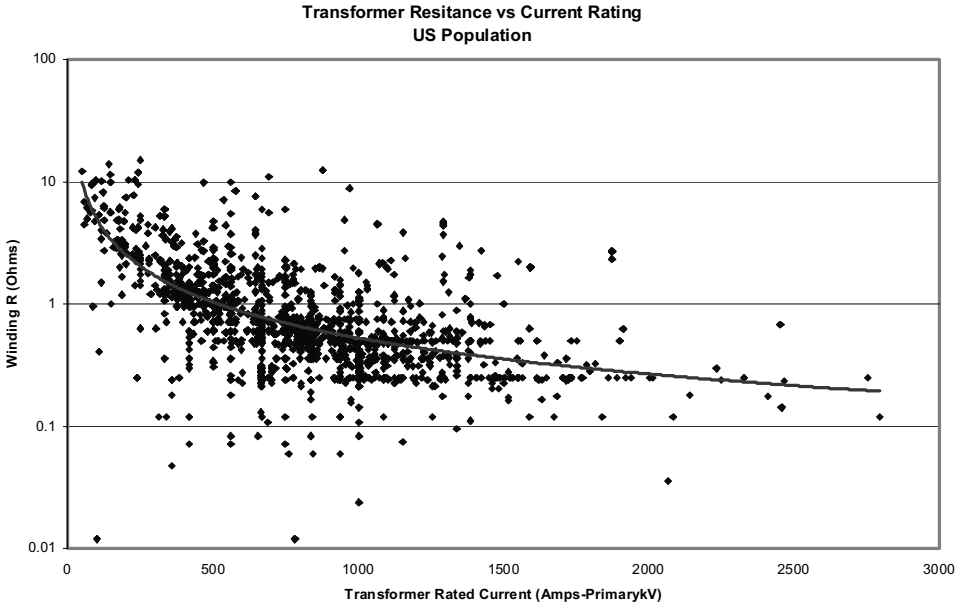

Figure 7. Statistics on average transformer resistive impedance versus AC current rating of the transformers in the US power grid population.

in the power grid resistances alone. Also for uniform comparison purposes, a 100 km long line is used in all kV Rating cases.

Figure 8 illustrates the comparison of GIC flows that would result for various US infrastructure power grid kV Ratings using the simple circuit and a uniform 1.0 volts/km geo-electric field disturbance. In complex networks, such as those in the US, some scatter from this trend line is possible due to normal variations in circuit parameters such as line resistances, etc that can occur in the overall population of infrastructure assets. Further, this was an analysis of simple "one-line" topology network, whereas real power grid networks have highly complex topologies, span large geographic regions, and present numerous paths for GIC flow, all of which tend to increase total GIC flows. Even this limited demonstration tends to illustrate that the power grid infrastructures of large grids in the US and other locations of the world are increasingly exposed to higher GIC flows due to design changes that have resulted in reduced circuit resistance. Compounding this risk further, the higher kV portions of the network handle the largest bulk power flows and form the backbone of the grid. Therefore the increased GIC-risk is being placed at the most vital portions of this critical infrastructure. In the US, 345kV, 500kV, and 765kV transmission systems are widely spread

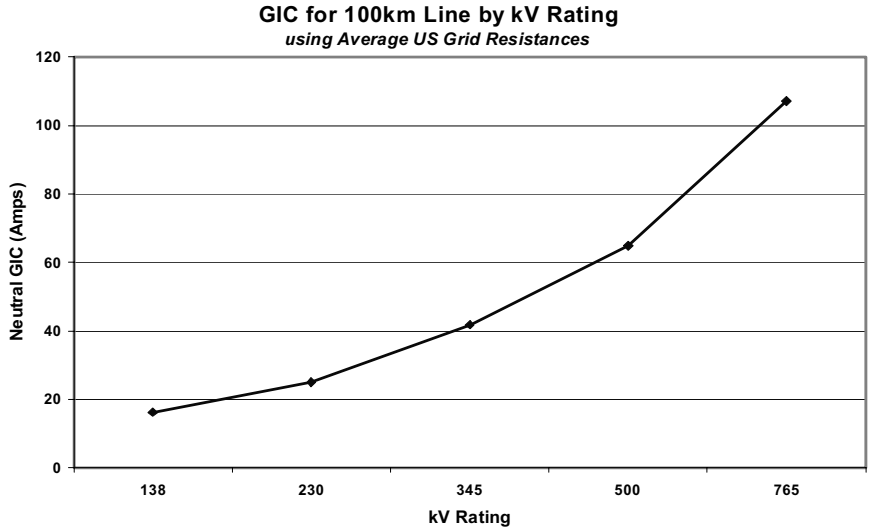

Figure 8**.** Average Neutral GIC Flows vs kV Rating for a 100km demonstration transmission circuit.

throughout the US and especially concentrated in areas of the US with high population densities.

One of the best ways to illustrate the operational impacts of large GIC flows is to review the way in which the GIC can distort the AC output of a large power transformer due to half-cycle saturation. Under severe geomagnetic storm conditions, the levels of Geo-Electric field can be many times larger than the uniform 1 Volt/km used in the prior calculations. Under these conditions even larger GIC flows are possible. For example in Figure 9, the normal AC current waveform in the high voltage winding of a 500kV transformer under normal full load conditions is shown (~300 amps-rms, ~400 amps-peak). With a large GIC flow in the transformer such as 195 amps, the transformer experiences extreme saturation of the magnetic core for one-half of the AC cycle (half-cycle saturation). During this half-cycle of saturation, the magnetic core of the transformer draws an extremely large and distorted AC current from the power grid. This combines with the normal AC load current producing the highly distorted asymmetrically peaky waveform that now flows in the transformer. As shown, AC current peaks that are present are nearly twice as large compared to normal current for the transformer under this mode of operation. This highly distorted waveform is rich in both even and odd harmonics, which are injected into the system and can cause mis-operations of sensors and protective relays throughout the network [Kappenman-1981, Kappenman-1989].

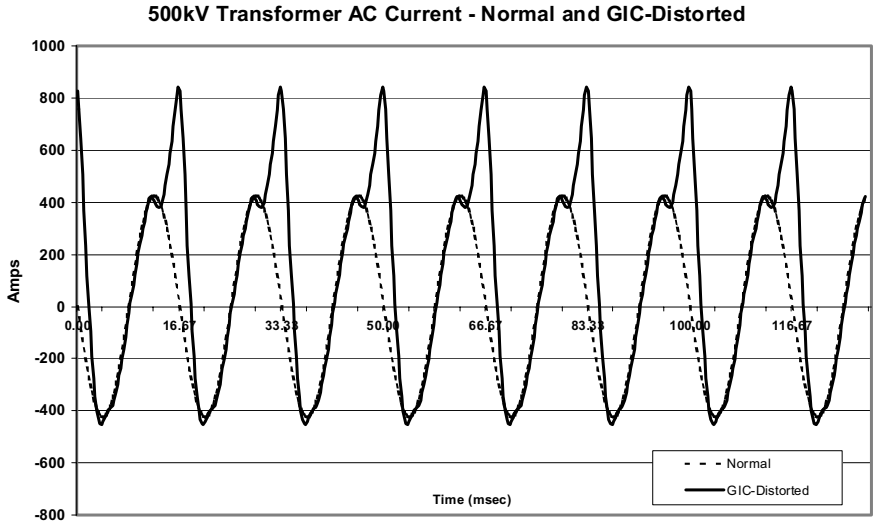

Figure 9**.** 500 kV Simple Demonstration Circuit Simulation Results –Transformer AC Currents and Distortion due to GIC.

All other transformers on the network can be exposed to similar conditions simultaneously due to the wide geographic extent of most disturbances. This means that the network needs to supply an extremely large amount of reactive power to each of these transformers or voltage collapse of the network could occur. The combination of voltage regulation stress, which occurs simultaneously with the loss of key elements due to relay mis-operations can rapidly escalate to widespread progressive collapse of the exposed interconnected network.

4. POWER GRID THREAT ASSESSMENT FOR GEOMAGNETIC STORM SCENARIOS

Geomagnetic disturbances have caused widespread disruptions to operation of power networks. Recent observations and analysis also indicate that GIC concerns for power grids are not exclusively confined to high-latitude locations. Geomagnetic storms present a number of processes that can drive impulsive or turbulent geomagnetic field variations at ground level. All of these disturbance processes can create conditions of complex and rapid expansions in geographic extent and intensity of impulsive geomagnetic field disturbances. As impacts to power networks can occur on a minute-by-

minute basis, these disturbance environments are not well-characterized by the current 3 hour planetary K, regional K, or any other geomagnetic storm indices that are available to operators of power networks. Rather, it is necessary to fully describe the complex physical manifestation of geomagnetic disturbance environments to model how and to what extent these disturbances impact modern ground-based critical infrastructures. However, the extremes of the impulsive geomagnetic disturbance environment are not well known on a regional basis at low, mid, and high latitude locations [Kappenman-2001].

Because power networks are too large and critical in their operation to easily perform physical tests of their reliability performance for various weather-caused contingencies, the ability to meet these requirements is commonly measured by deterministic study methods to test the power system's ability to withstand probable disturbances. Operators of these critical infrastructures perform extensive modelling and engineering analysis of risks to their systems in evaluating the design and expected performance of their systems for all conceivable operational threat scenarios, with the general exception of threats posed by space weather. These study methods rely extensively upon accurate simulation models of the network and the stress caused by the coupling and reaction to the threat environments. These environmental stress simulations are applied against the network under critical load or system stress conditions to define important system design and operating constraints on the network. System impact assessments for geomagnetic storm scenarios are a pressing need for operators of large complex power systems and if given sufficiently detailed environment data, these simulations can also be readily performed [Kappenman-2001, Albertson-1981, Pirjola-1985]. These advances in modelling have facilitated a number of power grids to begin a process of assessing and quantifying the power grid reliability risks posed by geomagnetic disturbances [Kappenman-2002]. The evaluation of power system vulnerability is, of necessity, a two-stage process. The first stage is one of assessing the exposure to the network posed by the impulsive geomagnetic field disturbances and the long-term climatology of these events specific to the end-user's region of interest. In other words, how large and how frequent can the storm driver be in a particular region? The second stage is one of assessment of the stress that storm events pose to reliability of operation. This is measured through estimates of levels of GIC flow across a network and the manifestation of impacts such as sudden and dramatic increases in reactive power demands and implications such as voltage regulation in the network for power grids. From this analysis effort, meaningful operational procedures can be further identified and refined to better manage the risks resulting from storms of various intensities [Kappenman-2001].

While techniques exist and are quite mature for simulating large-scale power system interaction with the geomagnetic storm environment, the key gap is in the capability to assess the climatology of geomagnetic storms and probable extremes of disturbance conditions in a form needed for systems concerned by GIC impacts. It is not only necessary to provide perspective on the frequency of geomagnetic superstorm events, but also on the extremes in magnitude that are possible. The analysis of historically important geomagnetic disturbance scenarios must take into account the three different and separate geomagnetic disturbance source regions and propagation processes;

i.) ionospheric electrojet intensifications and ground level propagation modes,

ii.) magnetopause/interplanetary boundary shocks and ground level propagation modes,

iii.) ring current intensification and ground level propagation modes.

Even when the geographic scope is limited in application to a country or region, the problem is still complex in that at all latitude locations, at least two of the three disturbance processes will exist.

5. EXTREME GEOMAGNETIC DISTURBANCE EVENTS – OBSERVATIONAL EVIDENCE

A number of new forensic investigations have been undertaken to evaluate storm events over the last 150 years, though modern indices such as Ap only extend back 70 years. These investigations indicate that several storms would far exceed the intensity of all storms over this 70-year period of Ap classification. One such example is a storm from September 1859. Using the Dst index as a measure of storm intensity, a comparison can be provided with the most recent Superstorm of the modern era, which occurred on March 13-14, 1989. For the March 89 Superstorm, the Dst reached a peak of –589. In comparison, the September 1859 storm is estimated to have reached a peak of -1760, a Mega-Storm intensity nearly 3 times larger than the March 1989 Superstorm [Tsurutani-2003]. Other storms, such as on May 1921, have produced measurable geo-electric fields that allow the ability to calibrate against more contemporary storm events. In the example of the May 1921 storm, geo-electric field intensities of ~20 V/km were observed, a level that is again over twice as large as those observed in both the March 1989 and July 1982 Superstorms [Elovaara-1992]. The fact that storms of such intensity as September 1859 and May 1921 have occurred before, indicate that they will eventually occur again. In the examination of these large storms, it is also the conclusion that the source solar event for these

Mega-Storms was not uniquely large and has been observed at intervals as often as once per decade. For example, the very large X22+ solar flare event observed on April 2, 2001 is a contemporary event and is estimated to be larger than the flare that triggered the 1859 storm [Tsurutani-2003]. Rather, what is important is the right convergence of factors from the Sun, to the solar wind and it's interaction with the Earth's magnetic field that set the framework for the Perfect Storm scenario. These Mega-Storms appear to be probable on a 1-in-50 to 1-in-100 year timeframe. Of course, modern critical infrastructures have not as-yet been exposed to storms of this size. Since GIC levels and GIC impacts tend to scale linearly with storm or geo-electric field intensity, it is reasonable to conclude that unprecedented levels of impacts are also likely for power grids and other infrastructures exposed to such extreme environments. More details on the threat to power grid infrastructures from such events will be provided in the following discussion of various storm processes of concern.

5.1 SSC's and Ring Current Intensifications – A New Facet of Space Weather Risk for Power Grids

Large impulsive geomagnetic field disturbances from auroral current systems have always been well understood as a concern for power grids in close proximity to these disturbance regions, predominantly at high-latitude locations. Magnetospheric shocks or SSC's due to large-scale interplanetary pressure pulses, are familiar from a geomagnetic disturbance perspective, but have not been understood in the context as a potential driver for large GIC's. Recent combinations of observational evidence and analysis are determining that such events are capable of producing equivalently large geo-electric fields and associated GIC risks at any latitude, even equatorial locations. Because of the small delta B magnitude observed at low-latitudes, such large GICs pose a paradox. A large SSC disturbance on March 24, 1991 produced some of the largest GIC's ever measured in the US, at mid-latitude locations.

The analysis methods and understanding of electromagnetic coupling processes at that time were unable to fully explain these observations. Figure 10 provides a comparison plot of the impulsive disturbance conditions observed for a typical electrojet-driven disturbance and the geomagnetic field disturbance from a large SSC event at a mid-latitude location. Large electrojet-driven disturbances can cause impulsive disturbances of 2000 nT or greater, while most SSC events are less than 200 nT (only 1/10th as large a disturbance) and could not be conceived as being capable of producing equivalently large geo-electric fields. Yet as shown in Figure 11, the resulting geo-electric fields from these two disturbances produce nearly equivalent intensity geo-electric fields [Kappenman-2003].

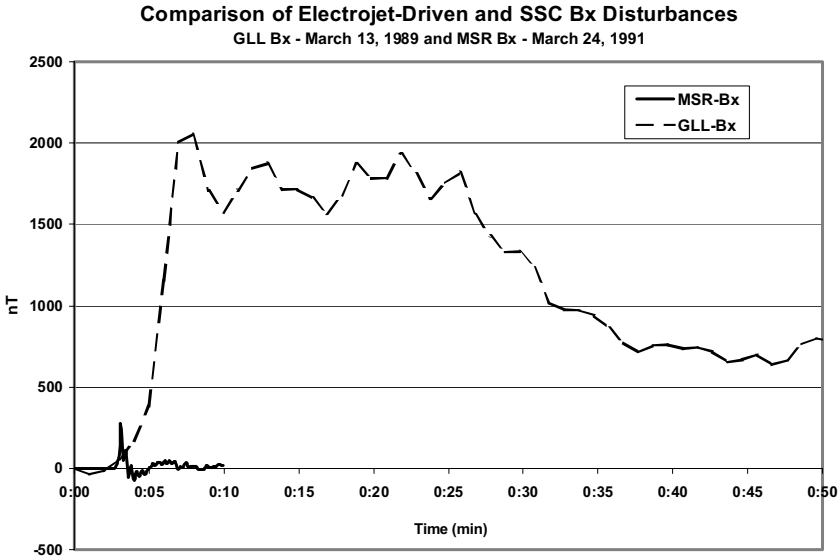

Figure 10. Comparison of delta Bx observed at GLL from electrojet-driven disturbance (March 13, 1989) and at MSR from SSC-event (March 24, 1991).

Electrojet-driven disturbances at high latitudes have large amplitude with relatively lower spectral content, while SSC events are characterized as low amplitude with extraordinarily high spectral content. Disturbance amplitude only accounts for part of the electromagnetic coupling process and the attribute of spectral content of the disturbance is equally important and heretofore had not been well understood and also not well measured unless high-cadence observations were conducted. The deep-earth ground conductivity also provides an important enabling role at higher frequencies. As previously noted, deep-earth ground response to geomagnetic field disturbances is both highly non-linear and highly frequency-dependent. As shown in Figure 12, for nearly all ground conditions, the higher the spectral content of the incident magnetic field disturbance, the higher the relative geo-electric field response. For SSC events, a proportionately smaller

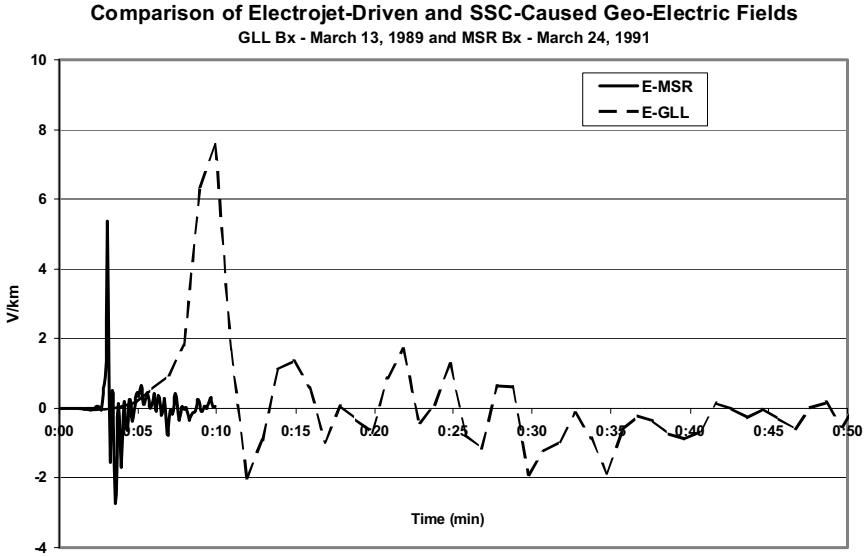

Figure 11**.** Comparison of estimated geo-electric field from Electrojet-driven disturbance as observed at GLL (March 13, 1989) and from SSC-event as observed at MSR (March 244, 1991).

magnitude but higher spectral content B field disturbance is capable of producing equivalent geo-electric fields due to the interaction with the more responsive frequency band of the ground models.

5.2 Ring Current Intensification Scenarios

Recent observations have determined that turbulent ground level geomagnetic field disturbances driven by intensification of the ring current can also create large GIC flows at low latitudes, which were confirmed by observations in central Japan [Erinmez-2002]. These disturbance events have been observed to produce GIC's of unusually long duration as well. These prolonged disturbance processes are driven by intensification of the equatorial ring current which has an equatorial location, as opposed to the electrojet current that has a higher latitude position. Because of the previously mentioned large excursions in Dst that are possible, a series of observations and simulations were conducted to estimate GIC magnitudes that are possible in the exposed 500kV grid of central Japan. Figure 13 provides a trend line projection compared to paired observations and calculations of GIC levels in the regional power grid. This trend line and

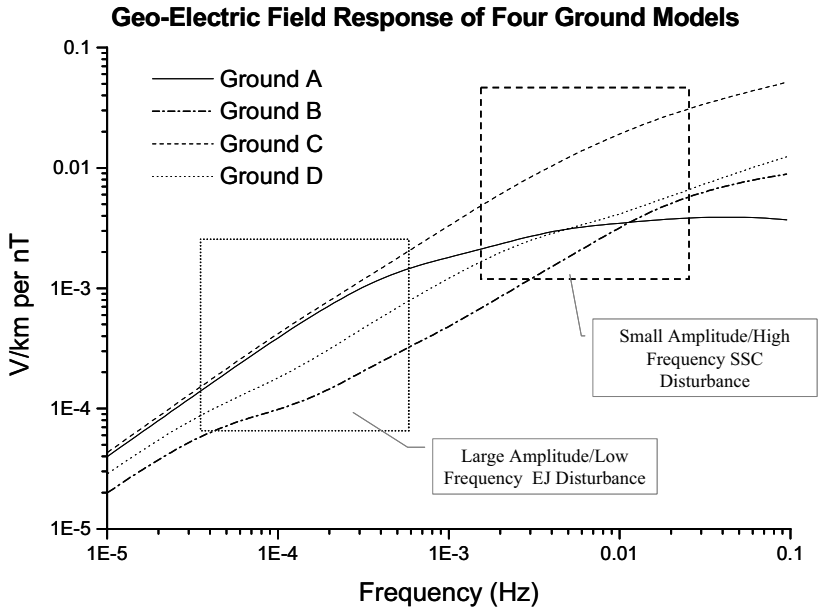

Figure 12. Interaction of large amplitude/low frequency electrojet disturbance and small amplitude/high frequency SSC disturbance with frequency-dependent characteristics of ground models.

companion simulations indicate GIC magnitudes at low latitude location power grids that could reach levels of 100 Amps of GIC for Dst levels reached during the March 13-14, 1989 Superstorm. The simulations utilized 1 second cadence magnetic observatory data, which is not available for a prospective Dst disturbance of ~1700. The high cadence observations provided sufficient spectral content details on the turbulent ground-level horizontal magnetic field disturbances during this storm. However, the observational details are not available for the speculative higher intensity storms such as that of September 1859. Therefore it is difficult to project with any certainty whether the trend line established in Figure 13 will also prevail to significantly higher Dst storm levels.

5.3 Electrojet Intensification Disturbance Scenarios

At high and mid-latitude locations, intensification of auroral or electrojet current systems in the ionosphere can produce very intense impulsive disturbance of the geomagnetic field over wide spread regions. It was predominantly these disturbance processes that triggered most of the power system disturbances over North America during the March 13-14, 1989 Superstorm.

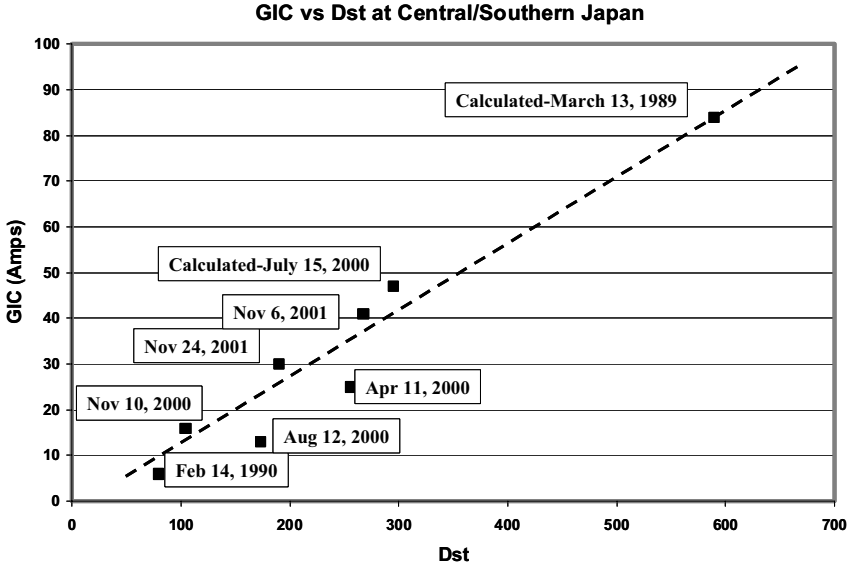

Figure 13. Trend of GIC flows and observed and calculated GIC flows in 500kV transformer in central Japan power grid due to ring current intensification at low latitude locations.

In addition to the Hydro Quebec blackout, the March 13-14, 1989 Superstorm caused numerous and widespread power system problems across North America. The NERC, in their post analysis, attributed over 200 significant anomalies across the continent to this one storm [NERC]. The intensity of the disturbance that triggered the Hydro Quebec collapse was at a level of 400 nT/min, while the most intense disturbance observed in North America was ~900 nT/min at the GLL observatory in southern Manitoba. In further assessing the disturbance intensities produced by this storm, the BFE observatory in Denmark observed the largest dB/dt with an intensity of ~2000 nT/min, a disturbance more than twice as intense than any experienced in North America [Kappenman-2001]. This observatory situated at ~50o geomagnetic latitude is at an equivalent latitude to mid-Atlantic regions across the US. Had this substorm erupted a few hours later, it would have been positioned over North America and could have caused a level of intensity that the power grids in the US have not faced in modern times. The last known disturbance approaching this level of dB/dt was observed over western portions of North America on August 4, 1972 [Anderson]. Less than 40% of the present-day power grid existed at that time and even smaller fractions of the extensive 500kV and 765kV grid that now extends across the US. The empirical experience from smaller intensity disturbances during the March 1989 storm over the US suggest such large disturbance events would

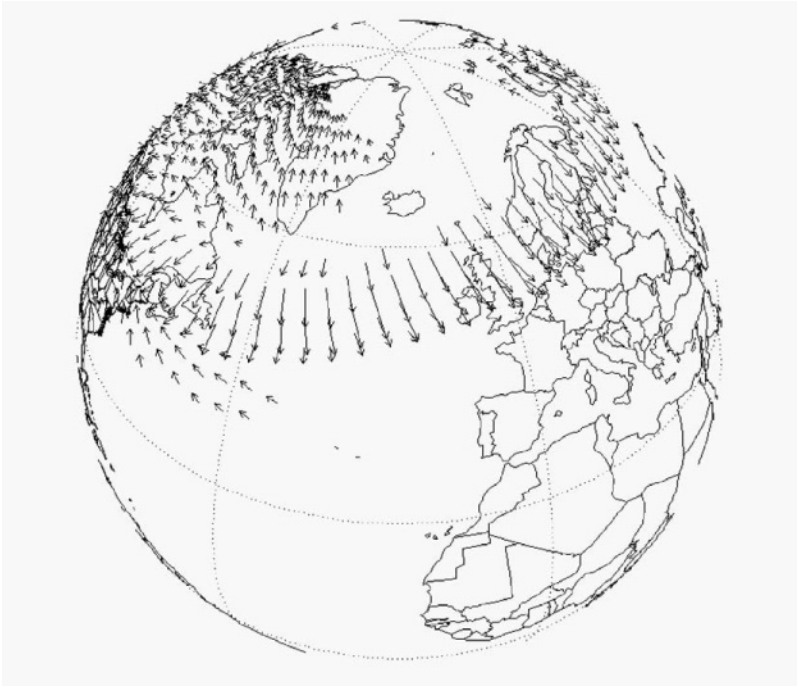

Figure 14. Extensive Westward Electrojet-driven geomagnetic field disturbances at time 22:00UT on March 13, 1989

have the potential to cause far greater power grid impacts in present day grids.

Data assimilation models provide further perspectives on the intensity and geographic extent of the intense dB/dt of the March 1989 Superstorm. Figure 14 provides a synoptic map of the ground-level geomagnetic field disturbance regions observed at time 22:00UT. The previously mentioned BFE observations are embedded in an enormous westward electrojet complex during this period of time. Simultaneously with this intensification of the westward electrojet, an intensification of the eastward electrojet occupies a region across mid-latitude portions of the western US. The features of the westward electrojet extend longitudinally ~120^{o} and have a north-south cross-section ranging as much as 5o to 10^{o} in latitude.

Older storms provide even further guidance on the possible extremes of these specific electrojet-driven disturbance processes. A remarkable set of observations was conducted on rail communication circuits in Sweden that extend back nearly 80 years. These observations provide key evidence that allow for estimation of the geomagnetic disturbance intensity of historically important storms in an era where geomagnetic observatory data is unavailable.

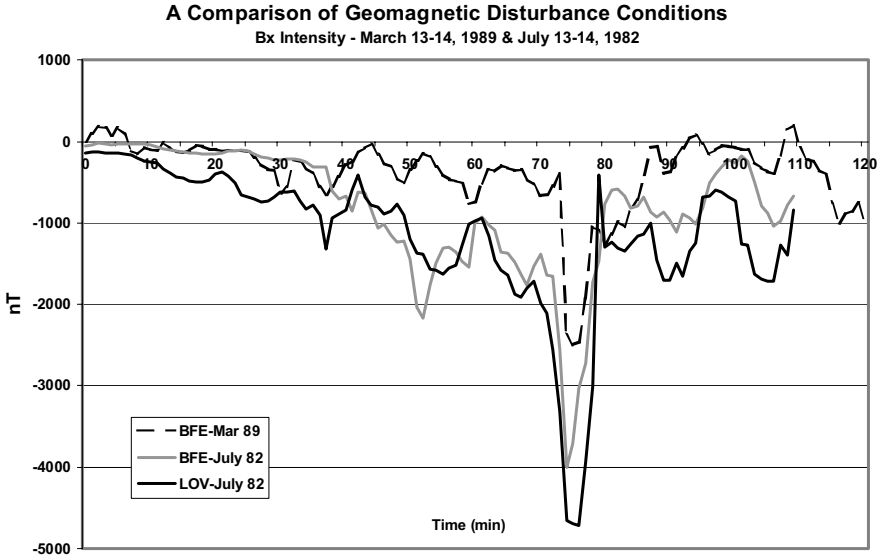

Figure 15. Comparison of observed delta Bx at Lovo and BFE during the July 13-14, 1982 and March 13, 1989 electrojet intensification events.

During a similarly intense westward electrojet disturbance on July 13-14, 1982, a ~100km length communication circuit from Stockholm to Torreboda measured a peak geo-potential of 9.1 V/km [Lindahl]. Simultaneous measurements at nearby Lovo observatory in central Sweden measured a dB/dt intensity of ~2600 nT/min at 24:00 UT on July 13. Figure 15 shows the delta Bx observed at BFE and Lovo during the peak disturbance times on July 13 and for comparison purposes the delta Bx observed at BFE during the large substorm on March 13, 1989. This comparison illustrates that the comparative level of delta Bx is twice as large for the July 13, 1982 event than that observed on March 13, 1989. The large delta Bx of >4000nT for the July 1982 disturbance suggests that these large field deviations are capable of producing even larger dB/dt impulses should faster onset or collapse of the Bx field occur over the region.

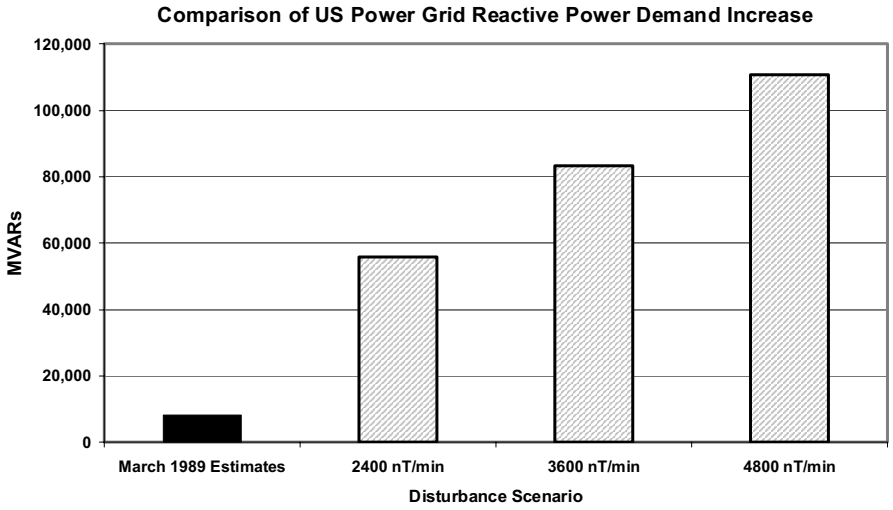

Figure 16. Comparison of estimated US power grid reactive demands during March 13, 1989 Superstorm and 2400, 3600, and 4800 nT/min disturbance scenarios at 50^{o} geomagnetic latitude position over the US.

6. US POWER GRID SIMULATIONS FOR EXTREME DISTURBANCE EVENTS

Based upon these extreme disturbance events, a series of simulations were conducted for the entire US power grid using electrojet-driven disturbance scenarios with the disturbance at 50^{o} geomagnetic latitude and at disturbance strengths of 2400, 3600, and 4800 nT/min. The electrojet disturbance footprint was also positioned over North America with the previously discussed longitudinal dimensions of a large westward electrojet disturbance. This extensive longitudinal structure will simultaneously expose a large portion of the US power grid.

In this analysis of disturbance impacts, the level of cumulative increased reactive demands (MVARs) across the US power grid provides one of the more useful measures of overall stress on the network. This cumulative MVAR stress was also determined for the March 13, 1989 storm for the US power grid, which was estimated using the current system model as reaching levels of ~7000 to 8000 MVARs at times 21:44 to 21:57UT. At these times, corresponding dB/dt levels in mid latitude portions of the US reached 350 to 545 nT/min as measured at observatories such as FRD, OTT and NEW. This provides a comparison benchmark that can be used to either compare absolute MVAR levels or, at a minimum, relative MVAR level increases for the more severe disturbance scenarios. The higher intensity disturbances of

2400 to 4800 nT/min will have a proportionate effect on levels of GIC in the exposed network. GIC levels more than 5 times larger than those observed during the above mentioned periods in the March 1989 storm would be a probable. With the increase in GIC, a linear and proportionate increase in other power system impacts is likely. For example, transformer MVAR demands increase with increases in transformer GIC. As larger GIC's cause greater degrees of transformer saturation, the harmonic order and magnitude of distortion currents increase in a more complex manner with higher GIC exposures. In addition, greater numbers of transformers would experience sufficient GIC exposure to be driven into saturation, as generally higher and more widely experienced GIC levels would occur throughout the extensive exposed power grid infrastructure.

Figure 16 provides a comparison summary of the peak cumulative MVAR demands that are estimated for the US power grid for the March 89 storm, and for the 2400, 3600 and 4800 nT/min disturbances at the different geomagnetic latitudes. As shown, all of these disturbance scenarios are far larger in magnitude than the levels experienced on the US grid during the March 89 Superstorm. All reactive demands for the 2400 to 4800 nT/min disturbance scenarios would produce unprecedented in size reactive demand increases for the US Grid. The comparison with the MVAR demand from the March 89 Superstorm further indicates that even the 2400 nT/min disturbance scenarios would produce reactive demand levels at all of the latitudes that would be ~6 times larger than those estimated in March 1989. At the 4800 nT/min disturbance levels, the reactive demand is estimated, in total, to exceed 100,000 MVARs.

This disturbance environment was further adapted to produce a footprint and onset progression that would be more geo-spatially typical of an electrojet-driven disturbance, using both the March 13, 1989 and July 13, 1982 storms as a template for the electrojet pattern. For this scenario, the intensity of the disturbance is decreased as it progresses from the eastern to western US. The eastern portions of the US are exposed to a 4800 nT/min disturbance intensity, while, west of the Mississippi, the disturbance intensity decreases to only 2400 nT/min. The extensive reactive power increase and extensive geographic boundaries of impact would be expected to trigger large-scale progressive collapse conditions, similar to the mode in which the Hydro Quebec collapse occurred. The most probable regions of expected power system collapse can be estimated based upon the GIC levels and reactive demand increases in combination with the disturbance criteria as it applies to the US power pools. Figure 17 provides a map of the peak GIC flows in the US power grid and estimated boundaries of regions that likely could experience system collapse due to this disturbance scenario.

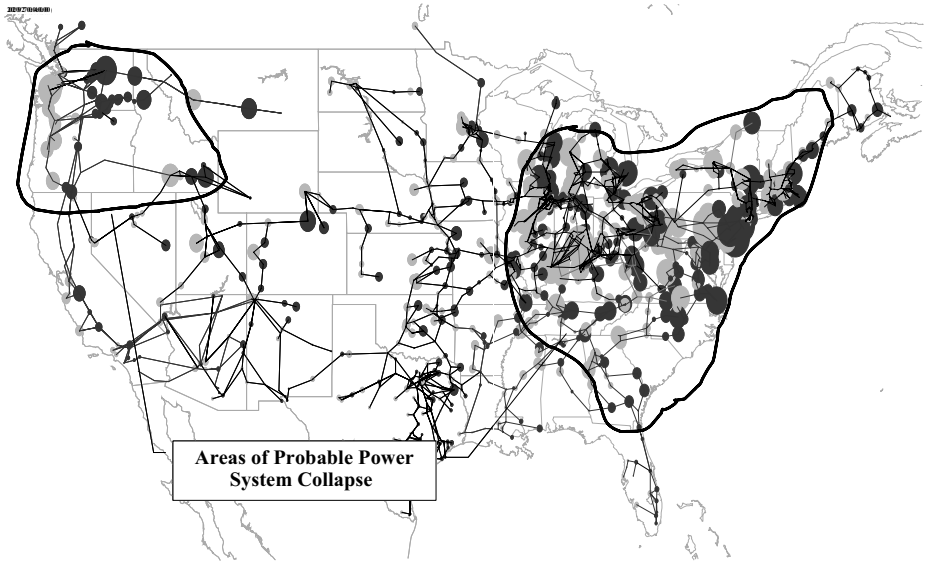

Figure 17. Regions of large GIC flows and possible power system collapse due to a 4800 nT/min disturbance scenario.

In addition to unprecedented levels of reactive power demands, the geographic region of possible power grid collapse is beyond any prior power industry experience with power grid failures, exceeding even the boundaries of the Great Northeast US Blackout of 1965. The 1965 blackout plunged major metropolitan areas of the US northeast (including Boston and New York City) into an extended blackout that lasted in excess of 12 hours duration before load restoration began. Both the size of the projected area of impact and the larger and more complex grid that exists today would present even greater obstacles in the grid restoration process. For an outage of this extent, the process of restoration and recovery could extend days, assuming minimal permanent damage occurs to the power grid infrastructure. The population within the above noted regions of collapse exceeds 100 million. This potential large-scale impact also raises legitimate concerns about the numerous interdependent infrastructures and vital public services that require electric power supplies. For instance in a timeline of only several hours of power supply outage, supplies of potable water for this large population become a concern. Within a day, this concern is further compounded by the probable loss of perishable foods.

7. CONCLUSIONS

Contemporary models of large power grids and the electromagnetic coupling to these infrastructures by the geomagnetic disturbance environment have matured to a level in which it is possible to achieve very accurate benchmarking of storm geomagnetic observations and the resulting GIC. As abilities advance to model the complex interactions of the space environment with the electric power grid infrastructures, the ability to more rigorously quantify the impacts of storms on these critical systems also advances. This quantification of impacts due to extreme space weather events is leading to the recognition that geomagnetic storms are an important threat that has not been well recognized in the past. These capabilities for detailed analysis and have also enabled the development of predictive tools to help the power industry deal with these threats.

New understandings of the complex nature of geomagnetic disturbance environments at low to high latitude locations and the increasing ability of grids of higher kV design to conduct large GIC flows are also changing the view of risks that power grids may face due to the space weather environment. It is no longer the case that power grids at high latitudes which are in close proximity to auroral electrojets are the only power systems that are *at-risk* due to GIC impacts. SSC and ring current intensifications can cause equivalently large GIC's in power grids located even at equatorial latitudes. Ultimately the combination of regional deep-earth ground conditions and the design of the power grid itself will determine the extent of possible GIC risk that will occur for a power system. The geo-electric field responses of regional ground conditions are highly uncertain, but all ground strata exhibit uniformly high degrees of frequency dependency and non-linear response across the frequency range of concern for geomagnetic disturbance environments. While more work is needed to better define the regional risk factors due to ground conductivity conditions, there is near unambiguous evidence that higher kV-Rated power grid designs are likely to experience relatively larger GIC flows for any geomagnetic disturbance condition or grid latitude location. The prevailing design evolution of power grids have greatly escalated this aspect of risk modifier as the power systems have grown in size and kV operating voltages. Because of this, kV rating is a more appropriate initial screening for determining GIC risk for power grids. In other words, power grids with operating voltage levels of 400kV or greater are all potentially at risk no matter where they may be located in the world.

Improving understanding of both storm processes and the interactions with power grid infrastructures are forcing a change in basic assessments of which power grids face risks from geomagnetic storms and for what reasons.

The risk implications extend to power grids that have never considered the risk of GIC previously because they were not at high latitude locations. In contrast to these previous notions, latitude location is not as important a consideration of GIC risk as that due to grid design and related risk factors. Both studies and observation evidence are indicating that power grids even at equatorial locations can have large GIC flows. In initial screening for determining GIC risk for power grids, operating voltage levels are proving to be a more relevant screening criterion. In other words, grids with operating voltage levels of 400kV or greater are all potentially at risk.

8. REFERENCES

Albertson, V.D., J.A. Van Baalen, Electric and Magnetic Fields at the Earth's Surface Due to Auroral Currents, *IEEE Transactions on Power Apparatus and Systems*, PAS-89, pg 578-584, 1970.

Albertson V. D., J. G. Kappenman, N. Mohan, G. A. Skarbakka, "Load-Flow Studies in the Presence of Geomagnetically-Induced Currents," *IEEE PAS Transactions*, Vol. PAS-100, February 1981, pp. 594-607.

Anderson, C.W., L.J. Lanzerrotti, C.G. Maclennan, Outage of the L-4 system and the geomagnetic disturbances of August 4, 1972, *Bell System Technology Journal*, 53, 1817, 1974.

Campbell, W. H., J. E. Zimmerman, "Induced Electric Currents in the Alaska Oil Pipeline Measured by Gradient Fluxgate and SQUID Magnetometers", *IEEE Transactions on Geoscience and Remote Sensing*, Vol. GE-18, No. 3, July 1980, pp. 244-250.

Campbell, W.H., Introduction to the Electrical Properties of the Earth's Mantle, *PAGEOPH*, Vol 125, Nos. 2/3, pages 193-204, 1987.

ECAR, How the Aging of Major Equipment Impacts Reliability, *ECAR Electric Equipment Panel Report*, 99-EEP-61, May 1999.

Elovaara J., et.al, Geomagnetically Induced Currents in the Nordic Power System and their Effects on Equipment, Control, Protection and Operation, *CIGRE* Paper 36-301, 1992 Session, 30 August - 5 September, 1992, Paris, 36-301, 11 pp., 1992.

Erinmez, I. A., S. Majithia, C. Rogers, T. Yasuhiro, S. Ogawa, H. Swahn, J. G. Kappenman, "Application of Modeling Techniques to assess geomagnetically induced current risks on the NGC transmission system", *CIGRE* Paper 39-304/2002-03-26, Paper presented at CIGRE 2002.

FERC, *FERC Form 1 Data*, US Federal Energy Regulatory Agency, Washington DC, 2000.

Howlett, R.D., T.K. Lungren, Bonneville Power Administration, Transformer Impedances, Transmission Impedances (345-138kV), 525 kV Transmission Impedances, *TOP-Network Planning System Electrical Data Book*, Revised 2002.

Kappenman J.G., V. D. Albertson, N. Mohan, "Current Transformer and Relay Performance in the Presence of Geomagnetically-Induced Currents," *IEEE PAS Transactions*, Vol. PAS-100, March 1981, pp. 1078-1088.

Kappenman J.G., D. L. Carlson, G. A. Sweezy, "GIC Effects on Relay and CT Performance," Paper presented at the EPRI Conference on Geomagnetically-Induced Currents, November 8-10, 1989, San Francisco, CA.

Kappenman, J.G., L. J. Zanetti, W. A. Radasky, “Space Weather From a User’s Perspective: Geomagnetic Storm Forecasts and the Power Industry”, *EOS Transactions of the American Geophysics Union*, Vol 78, No. 4, January 28, 1997, pg 37-45.

Kappenman J.G., “Geomagnetic Storm Forecasting Mitigates Power System Impacts,” *IEEE Power Engineering Review*, November 1998, pp 4-7.

Kappenman, J.G., Chapter 13 - “An Introduction to Power Grid Impacts and Vulnerabilities from Space Weather”, *NATO-ASI Book on Space Storms and Space Weather Hazards*, edited by I.A. Daglis, Kluwer Academic Publishers, NATO Science Series, Vol. 38, pg. 335-361, 2001.

Kappenman, J.G., SSC Events and the associated GIC Risks to Ground-Based Systems at Low and Mid Latitude Locations, *Paper submitted to AGU International Journal of Space Weather*, May 2003.

Lanzerotti, L.J., Geomagnetic induction effects in ground-based systems, *Space Sci. Rev.*, 34, pg 347-356, 1983.

Lindahl S, Swedish Railway Authority measurements from July 13-14, 1982. Personal communication from Sture Lindahl, May 22. 2002.

Masse, R.P., Crustal and Upper Mantel Structure of Stable Continental Regions in North America and Northern Europe, *PAGEOPH*, Vol 125, Nos. 2/3, pages 205-239, 1987.

NERC, “The 1989 System Disturbances” *NERC Disturbance Analysis Working Group Report*, “March 13, 1989 Geomagnetic Disturbance”, pp. 8-9, 36-60.

Pirjola, R., Estimation of the Electric Field on the Earth’s Surface during a Geomagnetic Storm, *Geophysica*, Vol. 20, No. 2, pp. 89-103, 1984.

Pirjola R., M. Lehtinen, “Currents produced in the Finnish 400kV power transmission grid and in the Finnish natural gas pipeline by Geomagnetically-induced electric fields”, *Annales Geophysicae* 3, 1985, pp. 485-491.

Rasmussen, T. M., R. G. Roberts, L. B. Pedersen, "Magnetotellurics along the Fennoscandian Long Range Profile," *Geophys. J. R. astr. Soc.*, Vol. 89, pp. 799-820, 1987.

Rasmussen, T. M., "Magnetotellurics in Southwestern Sweden: Evidence for Electrical Anisotropy in the Lower Crust?" *JGR* Vol. 93, No. B7, pp. 7897-7907, July 10, 1988.

Siscoe G.L., A Quasi-Self-Consistent Axially Symmetric Model for the Growth of a Ring Current through Earthward Motion from a Pre-Storm Configuration, *Planet. Space Sci.*, pp 285-295, Vol. 27, 1979.

Tsurutani, B. T., W. D. Gonzalez, G. S. Lakhina, and S. Alex, The extreme magnetic storm of 1–2 September 1859, *J. Geophys. Res.*, 108(A7), 1268, doi:10.1029/2002JA009504, 2003.